throughout the crystal, and so long as the electron diffusion length is more than a few atomic spacings, any charge-compensating center will be produced too far from the V^{2+} to affect it appreciably. This conclusion is confirmed by the experimental fact that no deviation from trigonal symmetry, such as would be produced by a neighboring defect off the c axis, is seen in the microwave[2] or optical spectrum.[3]

The case of Mn^{4+} is more complicated, as the charge-compensating center (Mg^{2+}) is introduced during growth and is necessary to produce the required charge state of manganese. While the microwave and optical spectra show the principal Mn^{4+} site to have trigonal symmetry,[4] the most likely place for the compensating Mg^{2+} ion is the nearest Al^{3+} site, which is on the c axis and therefore leaves the symmetry unaltered. There seems to be no evidence on this point though the view is sometimes expressed that the many weak lines observed in the optical spectrum to the blue of the R lines are due to locally charge-compensated sites.[15] The presence of local charge compensation not affecting the symmetry of the center would not affect the argument regarding the relative size of the "electronic" effect, as the contribution to V_u from the charge defect would affect the oscillator strength as well as the electric field splitting; it might affect the static local field correction, but surely not by a factor of 8. On the other hand, an exceptionally large "ionic" effect for Mn^{4+} could perhaps be due to a change in the nearest-neighbor geometry produced by a local defect. Thus, the present results are certainly consistent with, though they do not require, local charge compensation.

ACKNOWLEDGMENTS

I am grateful to Professor N. Bloembergen, Dr. P. S. Pershan, Dr. S. Geschwind, and Dr. D. L. Wood for helpful discussions; and to J. W. Ammons and K. A. Ingersoll for technical assistance.

[15] Four of these lines were studied at 4°K with an ac lock-in technique which permits the measurement of unresolved splittings. The lines at 14 908 and 14 914 cm^{-1} are split 18 ± 5 $cm^{-1}/(MV/cm)$; the line at 14 976 cm^{-1} is split 13 ± 2 $cm^{-1}/(MV/cm)$. The line at 15 087 cm^{-1}, which is much sharper than the others (it is 1 cm^{-1} wide at 4°K) is apparently not split, the limit of detection being 2 $cm^{-1}/(MV/cm)$.

PHYSICAL REVIEW VOLUME 133, NUMBER 3A 3 FEBRUARY 1964

Infrared Absorption of Magnesium Stannide

HERBERT G. LIPSON AND ALFRED KAHAN
Air Force Cambridge Research Laboratories, Office of Aerospace Research, Bedford, Massachusetts
(Received 27 August 1963)

Infrared transmission and reflection measurements have been made on n- and p-type semiconducting Mg_2Sn single crystals of different impurity concentrations between 2 and 30 μ, at temperatures ranging from 15 to 296°K. At incident energies less than 0.22 eV, strong free-carrier absorption is present; with α as the absorption coefficient and λ, the wavelength, this may be expressed as $\alpha=c\lambda^{3/2}$ at all temperatures where acoustical mode lattice scattering predominates. The absorption spectra due to other mechanisms has been analyzed after subtraction of the $\lambda^{3/2}$ free-carrier dependence. At energies of 0.22 eV and above, the rapid increase in absorption is attributed to the intrinsic edge. From the energy dependence of the absorption coefficient in the edge region, the mechanism of indirect transitions between the valence and conduction band can be established, with a phonon energy of 0.008 eV. A band in the 0.08 to 0.22 eV energy range present at all temperatures in n-type and above 196°K in p-type samples is interpreted in terms of transitions between two conduction band minima separated by 0.165 eV at 15°K. Below 0.06 eV an additional sharp rise in absorption occurs. A peak in this absorption at 26 μ may correspond to a second harmonic of the fundamental lattice vibration which is centered around 53 μ. An energy band picture for Mg_2Sn is suggested, and conductivity ($m_n^*=0.15m$, $m_h^*=0.10m$), and density of states ($m_n^*=1.2m$, $m_p^*=1.3m$) effective masses are calculated.

INTRODUCTION

MAGNESIUM stannide is a compound semiconductor of the II–IV series which crystallizes in CaF_2 structure, with Mg occupying the F^- sites and Sn occupying the Ca^{++} sites. This lattice is face-centered cubic with respect to Sn and contains a cube of eight atoms of Mg symmetrically located within the tin lattice. The electrical properties of Mg_2Sn have been the subject of a number of investigations,[1–3] but relatively little information is available on the optical properties[3,4] and their relation to the band structure.[5] With the acquisition of single crystals whose electrical measurements indicate high purity, an investigation of their

[1] U. Winkler, Helv. Phys. Acta. 28, 633 (1955).
[2] H. P. R. Frederikse, W. R. Hosler, and D. E. Roberts, Phys. Rev. 103, 67 (1956).
[3] W. D. Lawson, S. Neilsen, E. H. Putley, and V. Roberts, J. Electron. 1, 203 (1955).
[4] R. F. Blunt, H. P. R. Frederikse, and W. R. Hosler, Phys. Rev. 100, 663 (1955).
[5] J. Della Riccia, in *Proceedings of the International Conference on Semiconductor Physics, 1960* (Czechoslovak Academy of Science, Prague, 1961), p. 51.

infrared transmission and reflection spectra has been undertaken to extend the available data. This paper presents a detailed study of the temperature variation of the transmission of n- and p-type Mg_2Sn single crystals between 2 and 30 μ, from which further information on the band structure has been obtained.

Infrared absorption and photoconductivity measurements from liquid helium to room temperature made on p-type Mg_2Sn by Lawson *et al.*,[3] and on n- and p-type Mg_2Sn by Blunt *et al.*[4] have been interpreted in different ways, leading to widely different values for the energy gap and shift of the absorption edge with temperature. There is also a wide discrepancy in the values reported for the effective mass of Mg_2Sn. From thermoelectric power data on p-type samples Aigrain[6] obtained $m^*=0.14m$, electrical measurements[4] yielded $m_n^*=1.17m$ and $m_p^*=1.28m$, and from magnetic susceptibility experiments Korenblit and Kolesnikov[7] calculated $m_n^*=0.6m$. Optical measurements of both Lawson and Blunt indicate an absorption band in both n- and p-type Mg_2Sn with a peak at about 7.5 μ at room temperature. At low temperatures, this band was considerably reduced in n-type material, but it was not present in p-type. On the basis of their study of the latter, Lawson *et al.* suggest that this band is due to transitions within the valence band, while Blunt *et al.* offer the possibilities of absorption due to imperfections or lattice vibrations.

In view of its low-energy gap, intrinsic ionization occurs below room temperature in Mg_2Sn, and free-carrier absorption effects are of importance in determining the optical properties of this material. In this investigation, values of the forbidden energy gap, its temperature variation, and the phonon energy involved in the valence to conduction band transition were obtained from the absorption spectra after subtracting the effects of free carriers. From optical and electrical data, the conductivity and density of states effective masses have been calculated. The temperature variation and dependence on electron concentration of the 7.5 μ band are interpreted in terms of transitions within the conduction band. In addition, the presence of a fundamental lattice band and its second harmonic is indicated from measurements at longer wavelengths.

EXPERIMENTAL PROCEDURES

The Mg_2Sn single crystals used for optical measurements were chosen from crystals grown at this laboratory for stoichiometric studies.[8] The n- and p-type impurities resulted from the addition to the melt of excess Sn or Mg, respectively. Plane parallel surfaces of good optical quality were produced by polishing on a pitch lap.

Transmission and reflection measurements were made on these polished samples in the 2- to 30-μ range, using a Perkin-Elmer Model 112 spectrometer equipped with CaF_2, NaCl, KBr, and CsBr prisms. Measurements were made between liquid helium and room temperature, using an evacuated metal low-temperature Dewar equipped with NaCl and KRS-5 (thallium bromide-iodide) windows. To eliminate heating and possible emission effects produced by irradiation of the sample with the entire source spectrum, an optical arrangement was used by which the beam from the spectrometer exit slit could be imaged at a sample positioned inside the Dewar. The reflected or transmitted beam from the sample was then collected and imaged on an external thermocouple detector. Reflection measurements were made at an angle of incidence of approximately 8°. The Dewar was equipped with micrometer adjustments which allowed measurements of transmission or reflection by an in-out technique. The samples were mounted on Cu plates over one of two exactly matched apertures using G.E. 7031 cement, and these plates were clamped inside the Dewar for low-temperature measurements. For transmission, the remaining aperture was left open, while for reflection it was covered by an aluminum mirror used as a standard. Considerable care was exercised in attaching the sample and in preparing the mounting plates to avoid the possibility of strain.

The temperatures were obtained by using liquid helium, liquid nitrogen, dry ice, and ice as refrigerants. Temperatures close to that of the refrigerants were measured by clamping Cu-constantan thermocouples to the Cu plate, but thermocouples cemented to the plate or the sample, indicated the somewhat higher values of 15°K(He), 80°K(N_2), and 196°K(CO_2). The large window aperture of the Dewar necessary for comparative reflection measurements was assumed to be responsible for this higher sample equilibrium temperature. At helium temperature, an Au–Co, Au–Ag thermocouple which developed higher thermoelectric power was also used with one junction immersed in liquid helium. The thermocouple leads were inserted into the Dewar by an epoxy-sealed header, which eliminated spurious emf's.[9]

The sample thicknesses used for optical measurements were between 1.50 and 0.20 mm. Further reduction without cracking or disturbing the optical quality of the sample appears to be very difficult owing to the cleavage properties and softness of Mg_2Sn. Similar problems have been noted in the preparation of optical samples of other II–IV compounds.[10] Measurements of some thinner samples revealed a reduced transmission in the absorption edge; consequently, the data is not included in this investigation. Due to a limited amount of high purity material, no attempts were made to cleave plane parallel samples.

[6] P. Aigrain, Laboratoire Central des Industries Electriques, Final report Cont. AF-61(052)-138, AFCRC-TR-59-293 (unpublished).

[7] L. L. Korenblit and A. P. Kolesnikov, Zh. Tekhn. Fiz. **26**, 941 (1956) [translation: Soviet Phys.—Tech. Phys. **1**, 924 (1957)].

[8] B. D. Lichter, J. Electrochem. Soc. **109**, 819 (1962).

[9] H. G. Lipson and L. O. Bouthillette, Vacuum **13**, 145 (1963).

[10] P. Koenig, D. W. Lynch, and G. C. Danielson, Phys. Chem. Solids **20**, 122 (1961).

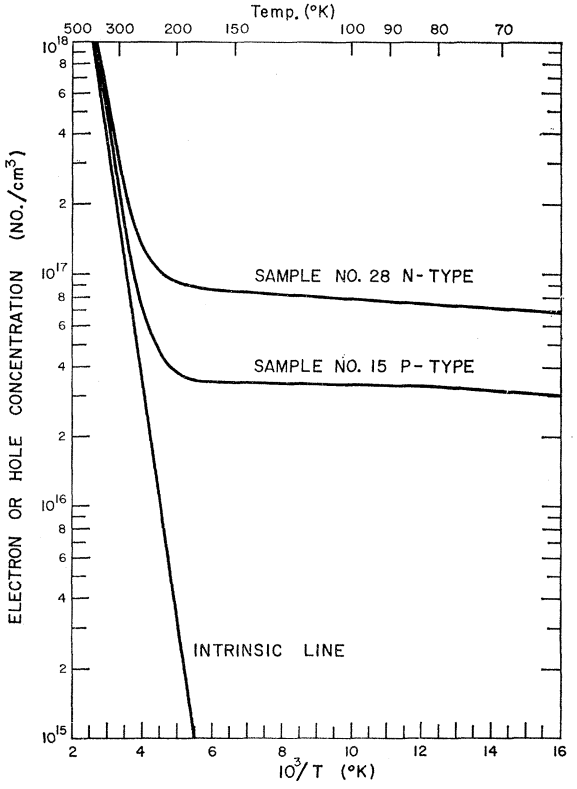

FIG. 1. Charge carrier concentration as a function of temperature of Mg_2Sn single crystals.

EXPERIMENTAL RESULTS

1. Electrical Properties

The Hall coefficient R_H and resistivity ρ between 60 and 300°K of the Mg_2Sn samples were measured by Lichter.[8] In the impurity region where either electrons or holes determine the conductivity, the carrier concentration n_e is related to the Hall coefficient R_H by $n_e=(3\pi/8e)(1/R_H)$. In the intrinsic range where both electrons and holes contribute to the conductivity, the carrier density has the form

$$n_e=\frac{3\pi}{8e}\left(\frac{b-1}{b+1}\right)\frac{1}{R_H}, \qquad (1)$$

where e is the electronic charge and b is the mobility ratio with a value of 1.20–1.25, as calculated from the p-type samples. The calculated carrier concentrations of representative n- and p-type samples of Mg_2Sn are shown in Fig. 1. As can be seen, the impurity densities, 10^{16}–10^{17} No./cm³, are of importance up to 200°K, while for temperatures above this value the intrinsic ionization becomes predominant. The carrier concentration values at the various temperatures used for the optical investigations are listed in Table I. In a subsequent calculation, we shall require the Hall mobility values of the n-type sample, and these as taken from Ref. 8 are also included in Table I. The energy gap at absolute zero temperature as calculated from the slope of the carrier concentration line of Fig. 1 yields a value of 0.35 eV. The impurity ionization energies are of the order of 0.005 eV for the p-type sample No. 15 and 0.010 eV for the n-type sample No. 28.

TABLE I. Carrier concentration and Hall mobilities as calculated from Hall coefficient and electrical conductivity.

Temp. (°K)	No. 28 n-type. $N_d=8.3\times10^{16}$/cm³				No. 15 p-type $N_a=3.4\times10^{16}$/cm³	
	n_e[a]	n_h[b]	n_h/n_e	μ_H[c]	n_e	n_h
296	2.7×10^{17}	1.8×10^{17}	0.67	130	1.8×10^{17}	2.1×10^{17}
273	1.8×10^{17}	9.0×10^{16}	0.46	180	9×10^{16}	1.2×10^{17}
196	8.9×10^{16}	4.0×10^{15}	0.045	525	4×10^{15}	3.8×10^{16}
80	7.5×10^{16}	...	...	2000	...	3.3×10^{16}

[a] n_e = density of electrons in the conduction band (/cm³)
[b] n_h = density of holes in the valence band (/cm³)
[c] μ_H = Hall mobility, cm²/V-sec.

For the determination of the effective masses m_n^* and m_p^* from electrical transport data, the parameter β, the variation of the energy gap with temperature, needs to be known. This quantity as calculated from the forbidden energy gap is $\beta=-3.2\times10^{-4}$ eV/°K resulting in $m_n^*=1.2m$ and $m_p^*=1.3m$. The energy gap, mobility, and effective mass values are in agreement with those reported by other investigators.[1,4]

2. Reflectivity Measurements

The reflectivity variation with wavelength measured at room temperature for representative n- and p-type samples is shown in Fig. 2. Values obtained by comparison of the sample reflectivity to that of an Al mirror were corrected for the reflectivity dependence with wavelength of an evaporated Al mirror. The small differences between the samples may be attributed to surface variations, and the over-all reflectivity level may be affected by the use of polished instead of cleaved surfaces. Distinct regions are apparent in Fig. 2. At the

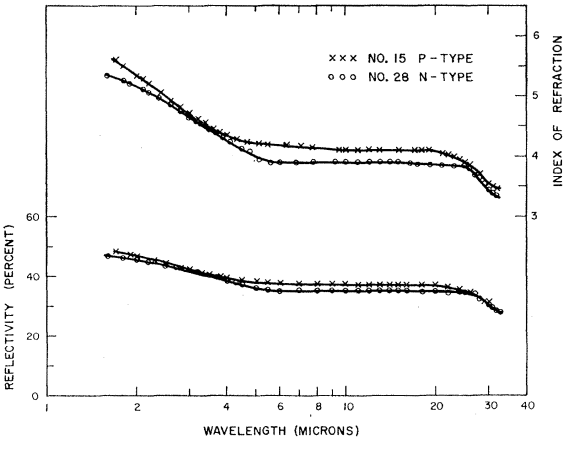

FIG. 2. Room-temperature reflectivity and index of refraction of Mg_2Sn as a function of wavelength.

shorter wavelengths corresponding to the absorption edge, as determined from the transmission data, reflectivity of both samples decreases with increasing wavelength until a relatively constant level of 35–37% is reached at 6 μ. This level is maintained up to approximately 22 μ, and at longer wavelengths the reflectivity of both samples again decreases. Measurements were also extended into the far infrared.[11] The general shape of the reflectivity curve between 22 and 65 μ shows the characteristics of reststrahlen reflection. The gradual decrease exhibited beyond 22 μ continues until a minimum is obtained in the vicinity of 41 μ, followed by a broad maximum at 53 μ. Due to the small size of the available samples, absolute values similar to those shown in Fig. 2 could not be determined with the far infrared equipment, but the reflectivity behavior confirms the results of McWilliams and Lynch.[12]

The index of refraction n is related to the extinction coefficient k and reflection coefficient R by

$$R=[(n-1)^2+k^2]/[(n+1)^2+k^2]. \quad (2)$$

It can be easily shown that for the condition of our experiments $k^2 \ll 1$, hence n can be determined from R alone:

$$n=(1+\sqrt{R})/(1-\sqrt{R}). \quad (3)$$

The calculated values of n are also shown in Fig. 2, and within the limits of the experimental data, they are in agreement with the values reported by McWilliams and Lynch.[13]

3. Absorption Coefficients

Plots of the absorption coefficient versus photon energy for a range of temperatures are shown for the

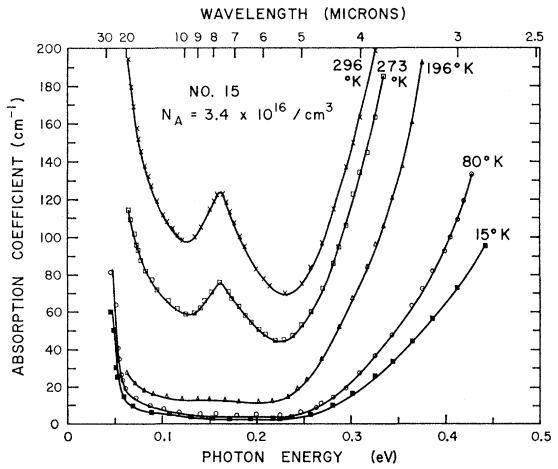

FIG. 3. Temperature dependence of absorption spectra of p-type Mg_2Sn.

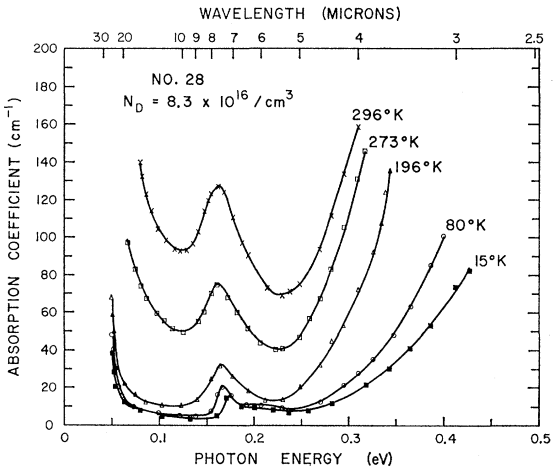

FIG. 4. Temperature dependence of absorption spectra of n-type Mg_2Sn.

p-type Mg_2Sn sample (Fig. 3) and for the n-type sample (Fig. 4). The values of the absorption coefficient α have been calculated from the formula[14]

$$T=\frac{I}{I_0}=\frac{(1-R)^2e^{-\alpha d}}{1-R^2e^{-2\alpha d}}. \quad (4)$$

Solving for the absorption coefficient

$$\alpha=-\frac{1}{d}\ln\left\{\frac{(1-R)^2}{2T}+\left[\left(\frac{(1-R)^2}{2T}\right)^2+R^2\right]^{\frac{1}{2}}\right\}, \quad (5)$$

where d is the sample thickness, and R is the reflectivity at the same wavelength at which transmission T is measured. The room-temperature reflectivity values of Fig. 2 have been used for absorption calculations at all temperatures.[15] The absorption values shown in Figs. 3 and 4 were obtained from transmission measurements on different sample thicknesses.

Between photon energies of 0.44 and 0.22 eV, the rapid increase in absorption coefficient is attributed to the intrinsic absorption edge. From 0.22 to 0.12 eV, an absorption band is observed at all temperatures for the n-type sample and at the higher temperatures for the p-type material. With increasing temperature, this band increases in strength and in the n-type sample the peak absorption also shifts toward lower energies. In the 0.12–0.06-eV region, the rise in absorption is characteristic of that of free carriers. Below 0.06 eV to the

[11] E. V. Loewenstein, AFCRL (private communication).
[12] D. A. McWilliams and D. W. Lynch, Phys. Rev. **130**, 2248 (1963).
[13] D. A. McWilliams and D. W. Lynch, J. Opt. Soc. Am. **53**, 298 (1963).
[14] H. Y. Fan and M. Becker, in *Proceedings of Reading Conference on Semi-Conducting Materials* (Academic Press Inc., N. Y., 1951), p. 132.
[15] A discussion of the derivation of Eq. (5) and a set of tables of αd as a function of T in intervals of 0.2% for parameters of R in 0.5% can be found in a report by A. Kahan and H. G. Lipson, AFCRL 63-325 (unpublished). The R used in this equation is the bulk reflectivity of the sample. Preliminary low-temperature measurements indicate that the bulk reflectivity variation with temperature is sufficiently small to justify the use of room-temperature reflectivity values at all temperatures.

limit of our data, an additional sharp rise can be seen at the lower temperatures.

DISCUSSION OF RESULTS

The absorption spectrum of a semiconductor is the result of a number of absorption mechanisms. In some energy regions the effects of several mechanisms are superimposed, introducing complications in the analysis of experimental data. For example, absorption due to the high free-carrier densities present in a low-energy gap semiconductor like Mg_2Sn can be large enough to mask the details of the intrinsic absorption edge and other bands. It is therefore desirable to separate and subtract the contribution of the free carriers from the total absorption. In the various energy regions, the curves of Figs. 3 and 4 have the characteristics of absorption attributed to: (1) free carriers, (2) valence to conduction band transitions, (3) transitions within the conduction band, and (4) lattice vibrations. A discussion of each of these effects will follow.

1. Free-Carrier Absorption

The free-carrier absorption, i.e., the absorption made possible by the carrier-lattice interaction, is dominant on the long wavelength side of the intrinsic absorption edge. In reference to Figs. 3 and 4, this would correspond to photon energies of 0.22 eV or less. It can be noticed that an additional absorption band masks the true behavior of the free-carrier absorption and consequently a comparison between the theoretical and experimental absorption coefficients will have to be restricted to photon energies of 0.12 eV and below.

The classical expression for the free-carrier absorption as predicted by the Drude-Zener theory is

$$\alpha_{f.c.}=\frac{1}{\pi}\frac{e^3}{m^2c^3}\left(\frac{m}{m^*}\right)^2\frac{n_e}{\mu n}\lambda^2, \tag{6}$$

where μ is the mobility, m^* the conductivity effective mass, and m the electronic mass. According to this equation, the absorption coefficient varies as λ^2, and in most n-type elemental and compound semiconductors this or higher power wavelength dependence is observed.[16]

The quantum mechanical treatment of lattice vibration and impurity scattering of conduction electrons has been discussed by Fan, Spitzer, and Collins.[17] The conductivity due to the interaction of free carriers and acoustical phonons is given as

$$\sigma=\frac{4}{9\sqrt{\pi}}\frac{\sigma_0}{\tau^2\omega^2}\left(\frac{\hbar\omega}{kT}\right)^{1/2}\left\langle\left(1+\frac{2E_k}{\hbar\omega}\right)\left(1+\frac{E_k}{\hbar\omega}\right)^{1/2}\right\rangle, \tag{7}$$

where σ_0 is the dc conductivity, $1/\tau$ the electron-lattice frequency, $\hbar\omega$ the incident photon energy, kT the electron thermal energy, and E_k the initial electron energy. Introducing the relationships for mobility $\mu=\sigma_0/en_e$, lifetime $\tau=\mu m^*/e$, and absorption coefficient $\alpha=4\pi\sigma/cn$, and after rearranging Eq. (7), we obtain the absorption coefficient due to free carriers:

$$\alpha_{f.c.}=\frac{4\sqrt{2}}{9\pi}\frac{e^3\hbar^{1/2}}{m^2c^{5/2}}\left(\frac{m}{m^*}\right)^2\frac{n_e}{\mu n}\frac{\lambda^{3/2}}{(kT)^{1/2}}\times\left\langle\left(1+\frac{2E_k}{\hbar\omega}\right)\left(1+\frac{E_k}{\hbar\omega}\right)^{1/2}\right\rangle. \tag{8}$$

It can be shown that for electrons obeying the classical distribution and for photon energies $\hbar\omega\gg kT$, the quantity in brackets to be averaged over the equilibrium energy distribution varies between 0.95 and 1.0, and for all practical purposes can be assumed to be unity. By the substitution of numerical values for the constants, Eq. (8) reduces to

$$\alpha_{f.c.}=\frac{1.47}{10^{17}}\frac{n_e}{(kT)^{1/2}}\left(\frac{m}{m^*}\right)^2\frac{\lambda^{3/2}}{\mu n}. \tag{9}$$

In the foregoing equation, λ is expressed in microns, kT in electron volts, and the mobility μ in cm^2/V-sec. A comparison of Eq. (9) with the classical Eq. (6) shows that the wavelength dependence of the absorption is changed from λ^2 to $\lambda^{3/2}$, and in addition a temperature dependence of $(kT)^{-1/2}$ is introduced.

A more general analysis by Meyer[18] for n-type Ge confirms the $\lambda^{3/2}$ dependence for $\hbar\omega/kT\gg1$ and predicts a λ^2 variation for $\hbar\omega/kT\ll1$. At room temperature $\hbar\omega/kT=48.5/\lambda$, and at liquid nitrogen temperature the relationship becomes $\hbar\omega/kT=185/\lambda$. The values of interest in the free-carrier investigations of Mg_2Sn range between 2.5 and 5.0 at room temperatures and between 10 and 20 at liquid-nitrogen temperature. Thus the incident photon energy to electron thermal energy ratio decreases with both wavelength and temperature. Then according to the quantum mechanical treatment, the intraband conduction electron absorption will behave as $\lambda^{3/2}$ at short wavelengths changing into a λ^2 dependence at longer wavelengths. In reality, if this behavior is not observed, the resulting absorption dependence is attributed to a combination of the acoustical and the higher power optical mode phonon scattering.

The preceding analysis is valid when the free-carrier absorption is caused by electrons only, i.e., at temperatures which are low enough to keep the hole to electron ratio small. An inspection of the data of Table I shows that at higher temperatures where intrinsic ionization becomes predominant this condition is not satisfied. It is assumed that the equation for the free-hole absorption is similar to that of Eq. (9) with $(n_e/\mu_n)(m/m_n^*)^2$ replaced by $(n_h/\mu_h)(m/m_h^*)^2$, the appropriate values ap-

[16] F. Stern, J. Appl. Phys. **32**, 2166 (1961).
[17] H. Y. Fan, W. G. Spitzer, and R. J. Collins, Phys. Rev. **101**, 566 (1956).
[18] H. J. G. Meyer, Phys. Rev. **112**, 298 (1958).

plicable to holes. The equation for the total free-carrier absorption, which is the summation of the two equations, can be simplified by the application of the expressions for the Hall coefficient

$$R_H=\frac{3\pi}{8e}\frac{n_h-b^2n_e}{(n_eb+n_h)^2}, \tag{10}$$

conductivity

$$\sigma=e(n_e\mu_n+n_h\mu_h), \tag{11}$$

and Hall mobility

$$\mu_H=R_H\sigma, \tag{12}$$

and becomes

$$\alpha=\frac{1.73}{10^{17}}\frac{n_e\lambda^{3/2}}{n\mu_Hb(kT)^{1/2}}\left(\frac{b^2-n_h/n_e}{b+n_h/n_e}\right)\times\left[\left(\frac{m}{m_n^*}\right)^2+b\frac{n_h}{n_e}\left(\frac{m}{m_h^*}\right)^2\right]. \tag{13}$$

The theoretical values of the absorption coefficient for the n-type sample No. 28 were calculated from Eq. (13) for the temperatures of 296, 273, 196, and 80°K, and plotted as the solid lines in Fig. 5. If the electrical data of Table I and the index of refraction of Fig. 2 are used, the values of $m_n^*=0.15m$ and $m_h^*=0.10m$ for the conductivity effective masses give the best correlation between the theoretically calculated and experimentally determined absorption coefficients. The experimental points are replotted in Fig. 5 and as can be seen, the data can be characterized by single valued effective masses. The curve for the 80°K temperature, to be discussed next, also includes the effects of impurity scattering. It can be noticed that at the short wavelengths the absorption deviates from the straight-line behavior as the other absorption mechanisms become important, and a similar effect can be observed at lower temperatures on the long wavelength side of the curves.

At low temperatures, the absorption due to impurities and lattice defects acting as scattering centers can become important. According to Fan *et al.*,[17] the equation for the absorption coefficient due to impurity scattering may be written as

$$\alpha_{\text{imp.}}=n_eN_i\left(\frac{m}{m^*}\right)^{3/2}\frac{\hbar^2e^6}{cm^{3/2}}\frac{Z^2}{n\epsilon^2}\times\frac{K_0(\hbar\omega/2kT)\exp(\hbar\omega/2kT)}{(kT)^{1/2}(\hbar\omega)^3}, \tag{14}$$

where N_i is the impurity concentration, Z is the number of charges on each ionized impurity center, and K_0 is the zeroth-order modified Bessel function. Evaluating the foregoing equation at 80°K, we find that on the average the value of the absorption coefficient attributed to impurity scattering is smaller by an order of magnitude as compared to that of lattice scattering. An initial comparison of the experimental data with the theoretically calculated lattice scattering coefficients did not give a satisfactory fit. However, as was pointed out by Meyer,[18] the previous equation underestimates the effect of the impurity scattering and for $\hbar\omega\gg kT$ this equation should be multiplied by the factor $(4\hbar\omega/\pi kT)^{1/2}$ which will raise the absorption coefficients to the same order as those due to lattice scattering. The curve for the 80°K temperature shown in Fig. 5 is the sum of the absorption due to both lattice and corrected impurity scattering, and satisfactory agreement results.

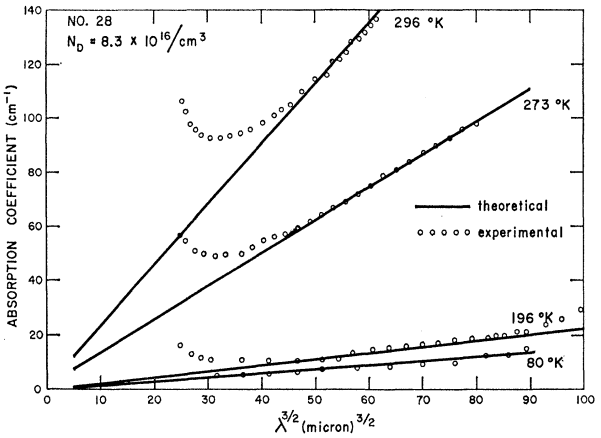

FIG. 5. Absorption coefficient as a function of $\frac{3}{2}$ power of wavelength at various temperatures. The solid lines are calculated from Eq. (13) using $m_n^*=0.15m$ and $m_h^*=0.10m$.

It was previously mentioned that the quantum mechanical $\lambda^{3/2}$ dependence of the absorption should change into the classical λ^2 variation at the longer wavelengths. This changeover, expected to occur at room temperature beyond 20 μ and at lower temperatures beyond 30 μ, is not observed in Mg_2Sn. Transmission measurements at room temperature at these wavelengths require very thin samples and, as discussed, considerable difficulty is encountered in the preparation of thin optical samples. At lower temperatures where the strong free-carrier absorption is not the limiting factor, the fundamental lattice band becomes predominant and its high power absorption masks the λ^2 dependence. To the best of our knowledge, n-type Mg_2Sn is the only semiconductor where acoustical phonon scattering and its $\lambda^{3/2}$ dependence is observed.

The $\lambda^{3/2}$ dependence is also satisfied at the longer wavelengths by the p-type sample. At temperatures above 80°K and at wavelengths less than 14 μ, an additional absorption proportional to the first power of the wavelength is superimposed on that due to the free carriers. An additional absorption with similar power and temperature dependence has been observed in p-type PbTe.[19] The $\lambda^{3/2}$ dependence of the free-carrier absorption was extended to longer and shorter wavelengths

[19] H. R. Riedl, Phys. Rev. 127, 162 (1962).

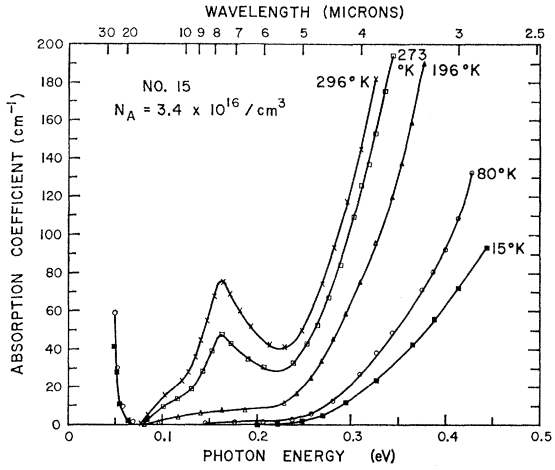

FIG. 6. Absorption spectra of p-type sample of Fig. 3 after subtraction of free-carrier absorption.

where other absorption mechanisms are present. The absorption versus energy plots of Figs. 6 and 7 were obtained by subtracting these free-carrier absorption values from the total absorption curves of Figs. 3 and 4.

2. Absorption Edge

The curves of Figs. 6 and 7 show the temperature dependence of the absorption edge and other bands for the p- and n-type Mg_2Sn. At higher energies the same absorption edge behavior is observed for both samples, but at lower energies the absorption edge tail is modified in a different manner by a band occurring beyond the edge. If the n-type sample, the effects of the band (which peaks at about 0.16 eV) are evident at all temperatures, while in the p-type, modification occurs only at higher temperatures. Also the additional absorption of the p-type sample above 0.08 eV, discussed in the previous section, raises the over-all level of absorption in this region.

Blunt *et al.*[4] determined the optical energy gap values from the intersection of the straight-line portion of the absorption edge curves with the energy axis and calculated the value of β, the shift of the energy gap with temperature. Extrapolation of the straight-line portions of the curves of Figs. 3 and 4 gives energy gap values ranging between 0.22 eV at 296°K and 0.30 eV at 15°K, and $\beta=-3\times10^{-4}$ eV/deg, in good agreement with Blunt. If the same procedure is applied to the curves of Figs. 6 and 7 from which the free-carrier absorption has been subtracted, higher energy intercept values are obtained at higher temperatures. Establishment of a single straight-line slope at any temperature in either Figs. 3 and 4, or Figs. 6 and 7, is difficult owing to the curvature of the absorption edge. Consequently, the determination of the energy gap and its shift with temperature from the intercept of the absorption curve with the energy axis is a questionable procedure in a low-energy gap semiconductor. Further, it is obvious that the value of the gap will depend on removal of absorption attributed to other mechanisms.

From analysis of the power dependence of the absorption edge, information on the energy gap and the type of transitions which occur between the valence and conduction bands of a semiconductor can be obtained. According to Smith,[20] McLean,[21] and others, the absorption follows the law of the form

$$\alpha h\nu=\sum_i A_i(h\nu-E_i)^n, \tag{15}$$

where $h\nu$ is the energy of the absorbed photon, and E_i is the valence to conduction band transition energy. If the absorption mechanism is due to indirect transitions between the bands, the exponent has the value $n=2$ when the direct transition is allowed, and $n=3$ when the direct transition is forbidden. These will be designated as indirect allowed, and indirect forbidden transitions, respectively. In Fig. 8, the $n=3$ relationship is plotted in the form $(\alpha h\nu)^{1/3}$ versus $h\nu$ using the absorption edge data of the p-type sample of Fig. 6. Aside from the absorption edge tail which is affected by the contributions of other bands, the data can be approximated by a series of straight lines. The slopes of these lines increase with temperature, and the intercepts on the energy axis show a consistent pattern, with values ranging from 0.19 eV at 15°K to 0.14 eV at 296°K. By a similar analysis Lawson *et al.*[3] obtain a straight-line dependence for the absorption edge but the slopes of the lines are such that a crossover occurs at 0.23 eV. As a result, the intercepts on the energy axis show opposite behavior in the sense that lower values are obtained at lower temperatures. This led them to the conclusion that in Mg_2Sn the energy gap increases with temperature and the transitions are of the indirect forbidden type. The crossover

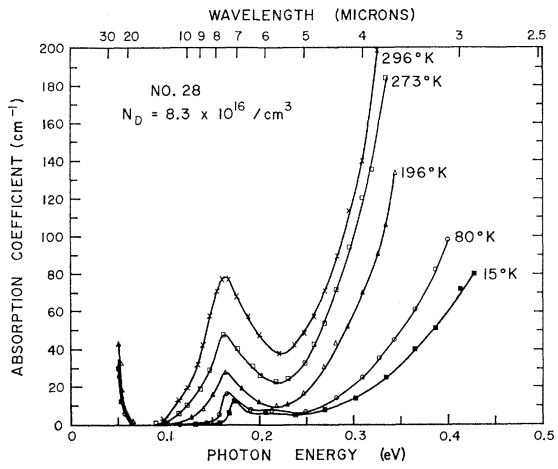

FIG. 7. Absorption spectra of n-type sample of Fig. 4 after subtraction of free-carrier absorption.

[20] R. A. Smith, *Semiconductors* (Cambridge University Press, London, 1959), p. 193.

[21] T. P. McLean, in *Progress in Semiconductors*, edited by A. F. Gibson (John Wiley & Sons, Inc., New York, 1960), **5**, p. 55.

of the curves and corresponding intercept values appear to be a result of the $a+b\lambda^2$ form of the free-carrier absorption subtraction used. If this method of free-carrier absorption subtraction is applied to our data, a similar reversal of intercept values occurs. Figure 9 presents the data of the p-type sample of Fig. 6 plotted in the form $(\alpha h\nu)^{1/2}$ versus $h\nu$, which describes the $n=2$ power dependence. Again a straight line fit is obtained from this power dependence, and the intercepts of the lines on the energy axis fall between 0.235 and 0.19 eV over the 15 to 296°K temperature range. When this analysis is applied to the absorption edge of the n-type sample of Fig. 7, both the $n=2$ and $n=3$ plots give, within the limits of the experimental data, slopes and intercept values identical to those of the p-type sample. As both the $n=2$ and $n=3$ relationships satisfy the linear power dependence, a clear-cut selection of the absorption mechanism cannot be made. However, it is evident that the band gap transitions are of the indirect type involving the absorption or emission or phonons.

In semiconductors where power dependence analysis has been applied, the absorption edge can be resolved into at least two distinct lines, corresponding to phonon absorption and emission. The intercepts of these lines with the energy axis can be used to determine the optical energy gap and phonon energies involved in the transition. If a single phonon process is involved, then Eq. (15) can be written as

$$\alpha h\nu=\frac{A(h\nu-E_g-E_{ph})^n}{1-\exp(-E_{ph}/kT)}+\frac{B(h\nu-E_g+E)_{ph}{}^n}{\exp(E_{ph}/kT)-1}, \quad (16)$$

where the first term gives the contribution from phonon emission, and the second from phonon absorption; A and B are constants and E_{ph} is the phonon energy. The temperature dependence of the slopes of the lines of Figs. 8 and 9 show that these plots represent phonon emission and hence the second term of Eq. (16) can be neglected. For the $n=3$ case, the data of Fig. 8 can be fitted by assuming the values of $A=2400$ and $E_{ph}=0.008$ eV, while for the $n=2$ case, the data of Fig. 9 can be fitted by assuming $A=885$ and $E_{ph}=0.008$–0.010 eV. Even though the $n=2$ power dependence cannot be fitted by a single phonon energy, the small variation in the calculated energy values does not warrant the exclusion of this mechanism. The phonon absorption slope is masked by other absorption mechanisms and a verification of the calculated phonon energy does not appear feasible. At the high absorption coefficient limit of our data, a second slope is discernible. This slope which is more prominent in the $n=2$ plots of Fig. 9 is noted by the dashed line. The authors agree with the remarks of Blakemore and Nomura[22] that the power dependence analysis of the absorption edge of low energy gap semiconductors is a frustrating proposition.

From Eq. (16), the indirect energy gap of a semiconductor is the energy axis intercept of the phonon emission line less the calculated phonon energy. Values of this gap as a function of temperature, designated as

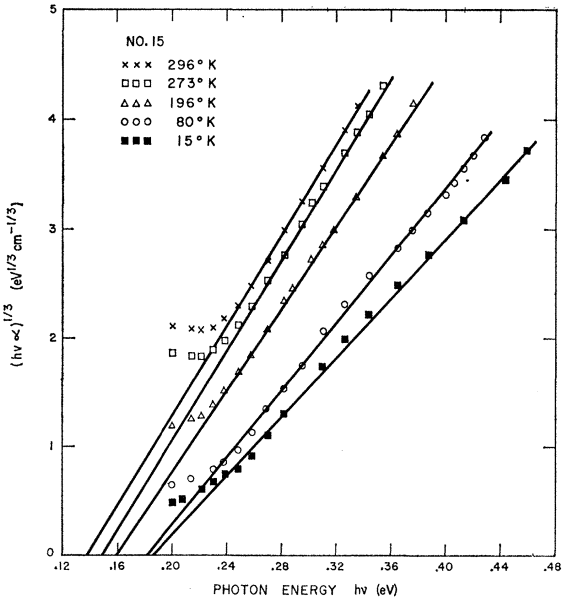

FIG. 8. Power dependence ($n=3$, corresponding to indirect forbidden transition) of absorption edge data of Fig. 6.

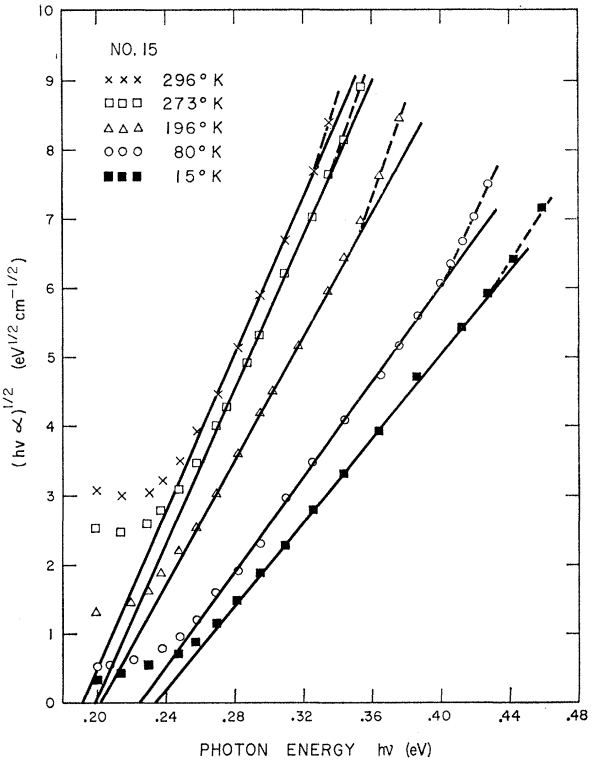

FIG. 9. Power dependence ($n=2$, corresponding to indirect allowed transition) of absorption edge data of Fig. 6.

[22] J. S. Blakemore and K. C. Nomura, Phys. Rev. **127**, 1024 (1962).

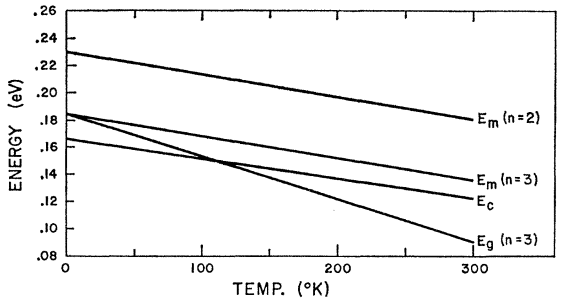

FIG. 10. Mg_2Sn energy gaps as a function of temperature; E_m is the transition energy between the top of the valence band and the lowest unfilled level of the conduction band; E_c the threshold energy for transitions within the conduction band; and E_g the indirect energy gap (see Fig. 14).

E_m, are shown in Fig. 10 for both the $n=2$ and $n=3$ cases. The gap values for both indirect allowed and indirect forbidden transitions are shown, as no selection between the two mechanisms can be justified, as previously stated. The energy gaps at absolute zero and room temperature for $n=2$ are: $E_0=0.23$ eV and $E_{296}=0.18$ eV; for $n=3$, $E_0=0.185$ eV and $E_{296}=0.135$ eV. The shift of the energy gap with temperature, with a value of $\beta=-1.7\times10^{-4}$ eV/deg, is the same for both cases. In the following section we shall reconsider whether these values truly represent the parameters.

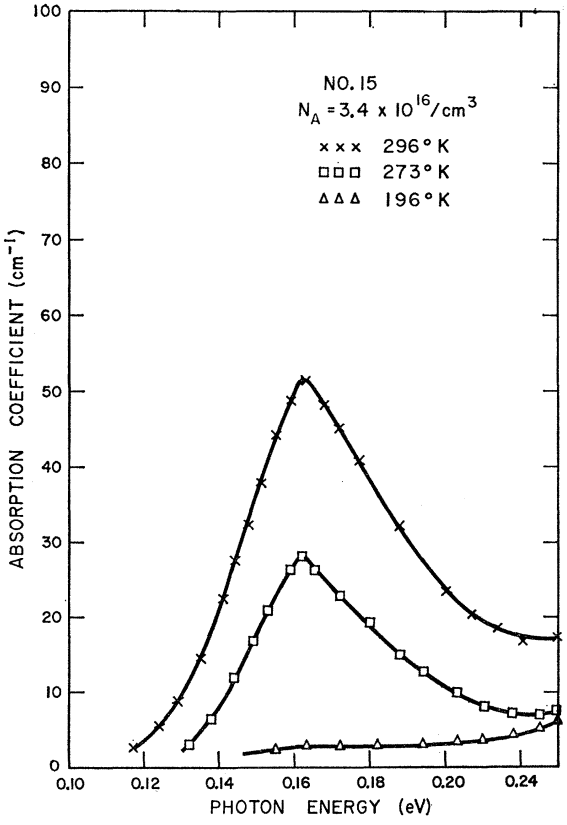

FIG. 11. Resultant band in p-type Mg_2Sn for various temperatures after subtracting free carrier and additional absorption.

3. Absorption Bands

An examination of Figs. 6 and 7 reveals a strong absorption band in the 0.08–0.22-eV energy range. As previously discussed, an additional absorption proportional to the first power of the wavelength is present in the p-type sample. To allow a direct comparison of this band in both the n- and p-types, the straight line representation of this additional absorption on a logarithmic plot has been extended to shorter wavelengths and these values, along with those of the free carriers, subtracted from the total absorption. The resultant absorption, and a plot of the band of the n-type sample of Fig. 7, are shown on the same scale in Figs. 11 and 12. The peak value of the band of the n-type sample shifts to lower energies with increasing temperature. This occurs principally when impurity ionization predominates; above 196°K where the main contribution of electrons to the conduction band stems from intrinsic ionization, there is no appreciable shift. Between 15 and 196°K the shift of the peak is approximately 0.010 eV, as indicated by the dotted line in Fig. 12. In the n-type sample, an additional broad low level absorption is evident at the lower temperatures above 0.19 eV. The asymmetrical shape of the absorption band can be attributed to the proximity of the intrinsic absorption edge tail.

From a comparison of the absorption curve at each temperature with the electron concentration in Table I, it is apparent that the band is related to the density of electrons in the conduction band. The absorption begins to appear in the p-type sample at temperatures above 196°K when electrons are present in the conduction band due to intrinsic ionization, while in the n-type sample where electrons result from both impurity and intrinsic ionization, the band occurs at all temperatures. In Fig. 13, the maximum absorption values of the band for both samples are plotted as a function of electron concentration. The low-level absorption observed above 0.19 eV at the two lower temperatures in the n-type sample introduces some uncertainty in the determination of the peak value. Nevertheless, within the accuracy of the absorption measurements and the carrier concentration values, all points lie close to a straight line of unit slope, indicating that the peak of the band is proportional to electron density. The threshold energies of the absorption band of Figs. 11 and 12 at each temperature can be approximated from the extension of the steep slopes of the curves on the low-energy side of the absorption peak. The energies as a function of temperature, designated as E_c, are shown in Fig. 10. These energies decrease with increasing carrier concentration, having the values 0.165 eV at 15°K and 0.12 eV at 296°K. The slopes of the absorption edge of this band as determined from a logarithmic plot decrease with increasing temperature and imply an indirect transition mechanism.

Although the possibility still remains that the absorption band can be attributed to a deep lying impurity

present in all samples, the absence of any discernible steep slope in the Hall coefficient data and the proportionality of absorption with electron concentration point to an alternate explanation in terms of conduction band transitions. In particular, the absence of any band in the p-type material at temperatures below that of intrinsic ionization supports this interpretation. Conduction band transitions have also been proposed for a similar absorption band observed in Si,[23] GaAs,[24], AlSb,[25] and another II–IV compound, Mg_2Si.[10]

A schematic energy band diagram consistent with the previously discussed experimental results is depicted in Fig. 14. Based on the power dependence of the absorption edge, the valence to conduction band transitions

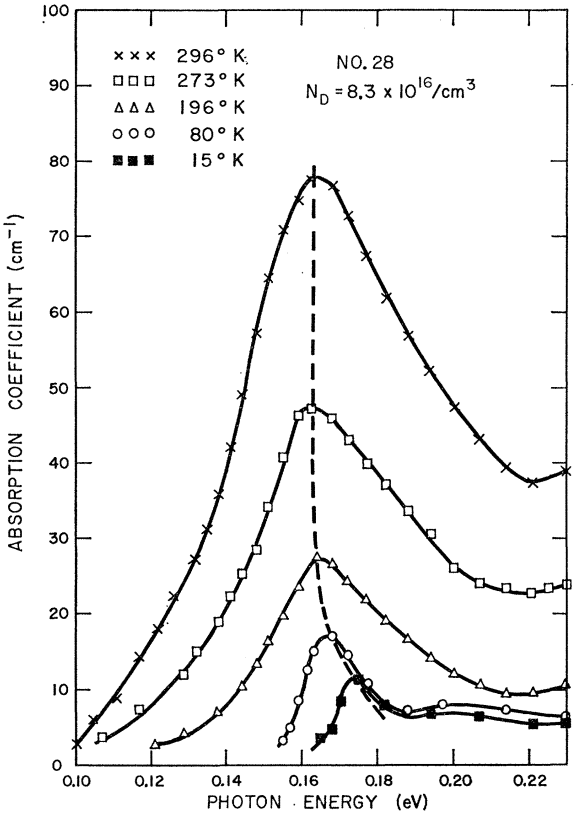

FIG. 12. Expanded plot of absorption band for various temperatures in n-type Mg_2Sn (data of Fig. 7). The dashed line shows shift of band peak with temperature.

are indirect with the conduction band minimum not necessarily at the zone edge. The transitions responsible for the absorption band are shown to occur between the top levels of this conduction band and the higher lying minimum. Even though the transition is indicated as indirect, the mechanism of a direct transition between the conduction bands cannot be excluded. The separation of the minima as indicated by the threshold energy

[23] W. G. Spitzer and H. Y. Fan, Phys. Rev. **108**, 268 (1957).
[24] W. G. Spitzer and H. Y. Fan, Phys. Rev. **114**, 59 (1959).
[25] W. J. Turner and W. E. Reese, Phys. Rev. **117**, 1003 (1960).

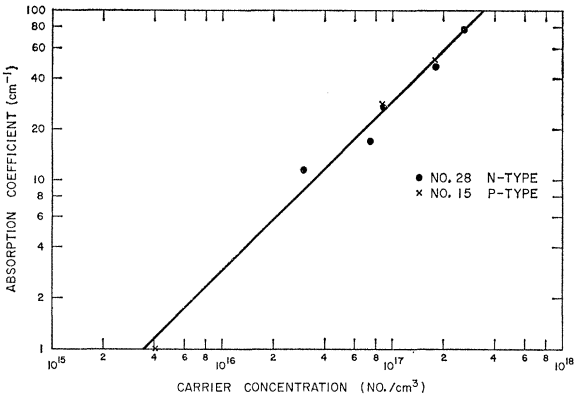

FIG. 13. Absorption band peak as a function of electron concentration in the conduction band. The solid line is of unit slope.

is 0.165 eV at absolute zero. The variation of the threshold energy for the conduction band transition can be explained by the rise of the Fermi level with electron concentration. The shift of the absorption peak from 0.165 to 0.175 eV is due to the added energy of a donor impurity level $E_i = 0.010$ eV below the conduction band. This is also the value of the impurity ionization energy estimated from Hall coefficient data. The valence band is assumed to have the conventional triple degeneracy at $k=0$, and from the inversion symmetry characteristic of a face-centered cubic structure the lower valence band is split off by spin-orbit interaction. The separation of the valence band maxima has the value of 0.08 eV, as determined from the onset of the additional absorption of the p-type sample shown in Fig. 6. This occurs in the p-type sample No. 15 above 196°K, but is also observed at lower temperatures in material with higher acceptor concentrations. With an energy band scheme of this type, the variation in the effective mass values resulting from different experiments is not too surprising.

In view of the variation of the threshold energy, the

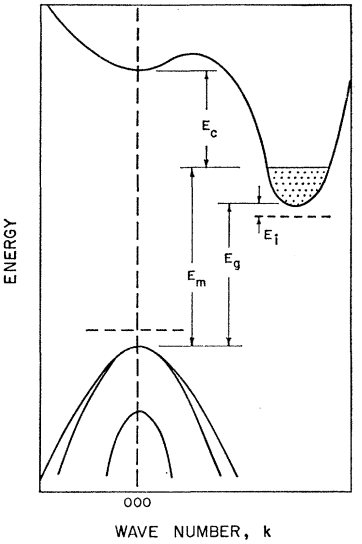

FIG. 14. Suggested energy band picture for Mg_2Sn.

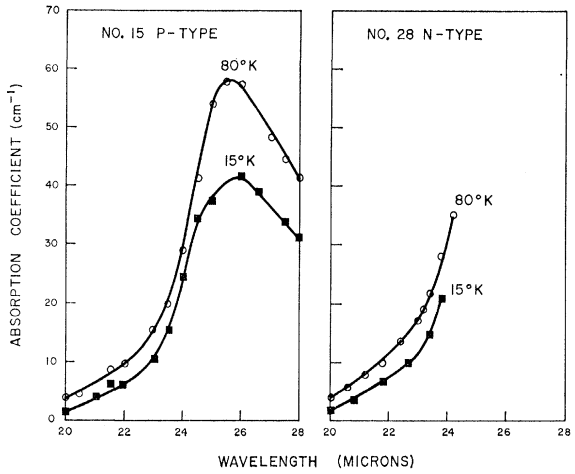

FIG. 15. Lattice vibration absorption as a function of wavelength in Mg_2Sn.

question arises: Does the indirect energy gap, calculated in the previous section from the power dependence of the absorption edge, represent the separation of the top of the valence band and the minimum of the conduction band, or the distance from the top of the valence band to the filled level of the conduction band? In the latter case, the indirect energy gap would be given by $E_g=E_m-[E_{c(T=0)}-E_{c(T)}]$; Fig. 10 shows this gap for $n=3$ as a function of temperature. The energy gap value at absolute zero temperature is unaffected but the room-temperature value decreases to 0.09 eV, and correspondingly β increases from -1.7×10^{-4} to -3.2×10^{-4} eV/°K. The identical value of β and a room temperature E_g value of 0.135 eV is found from the $n=2$ slope. If the indirect forbidden transition mechanism is accepted as the proper one, the value of the direct energy gap at 0°K is the sum of the indirect gap (0.185 eV) and the conduction band transition (0.165 eV), yielding 0.350 eV in agreement with the value calculated from the electrical data. On the other hand, there are indications which favor the indirect allowed mechanism. As mentioned, in reference to Fig. 9, at the high-energy limit of our data a second steeper slope is discernible. This slope could correspond either to a second phonon emission, or to the onset of the direct transition from the valence band to the higher lying conduction band minimum. Considering data of both p- and n-type samples, one finds at all temperatures reasonable agreement between the energy value at which this second slope appears and the calculated value for the direct transition.

4. Lattice Vibrations

After subtraction of the free-carrier contribution, the absorption which remains at longer wavelengths is plotted at the two lowest temperatures for the p- and n-type samples in Fig. 15. This subtraction is performed by representing the extension of the free-carrier contribution and the total absorption on a logarithmic scale. By this method the effects of both impurity scattering, the dominant free-carrier mechanism at the low temperatures, and the lattice scattering have been removed. From the rapid rise in absorption beyond 20 μ accompanied by a decrease in reflectivity in this same spectral region (Fig. 2), it was concluded that Mg_2Sn has a fundamental lattice vibration at longer wavelengths.[26] As previously mentioned, extension of the reflectivity data to longer wavelengths confirms the presence of a fundamental lattice vibration band centered around 53 μ. From the curves of Fig. 15, it appears that the strength of the absorption does not depend on carrier concentration or type, as would be expected in the case of lattice vibration absorption. In the p-type sample where measurements were carried out to 28 μ, a peak in the absorption occurs at 26 μ. If the peak of the fundamental lattice vibration absorption as determined by reflectivity data occurs at 53 μ, a second harmonic may be observed at 26.5 μ. The absorption peaks of Fig. 15 could correspond to this second harmonic. Modification of the present far infrared equipment to obtain reflectivity measurements on small samples with higher resolution is in progress. A determination of absolute reflectivity values should clarify the lattice vibration spectra and allow the application of classical dispersion theory to Mg_2Sn.

ACKNOWLEDGMENTS

The authors are indebted to Dr. B. D. Lichter (now at the University of California at Berkeley) for growing the samples and for many stimulating discussions. Their appreciation is expressed to Mr. L. Bouthillette for help in the experimental phases of the work, to Mr. E. Brown for performing the computations, and to Miss O. Denniston for assistance in preparation of the paper. Thanks are due also to Professor M. Balkanski, University of Paris, for helpful suggestions, to Dr. D. Warschauer, Raytheon Research Laboratory, for valuable criticism, and to Dr. E. Czerlinsky, AFCRL, for continued support of this work.

[26] H. G. Lipson, Bull. Am. Phys. Soc. 8, 144 (1963).